Powder Technology 305 (2017) 125–131

Contents lists available at ScienceDirect

Powder Technology

journal homepage: www.elsevier.com/locate/powtec

Ultrafine clarithromycin nanoparticles via anti-solvent precipitation in subcritical water: Effect of operating parameters

Yuan Pu [a,b], Xiaofei Wen [a], Yinhua Li [a], Dan Wang [a,b,*], Neil R. Foster [a,c], Jian-Feng Chen [a,b]

[a] State Key Laboratory of Organic-Inorganic Composites, Beijing University of Chemical Technology, Beijing 100029, China
[b] Research Center of the Ministry of Education for High Gravity Engineering and Technology, Beijing University of Chemical Technology, Beijing 100029, China
[c] Department of Chemical Engineering, Curtin University, Perth, Western Australia 6102, Australia

ARTICLE INFO

Article history:
Received 13 June 2016
Received in revised form 16 August 2016
Accepted 27 September 2016
Available online 28 September 2016

Keywords:
Clarithromycin
Subcritical water
Bioavailability
Nanoparticles
Nanocomposites

ABSTRACT

Clarithromycin (CLA) is an important drug used to treat various bacterial infections, while its effective bioavailability is limited by the poor water-solubility of the CLA molecule. Subcritical water (SBCW) processes have been demonstrated to be a new promising alternative for the preparation of drug nanoparticles with enhanced dissolution rate. In this work, we reported ultrafine CLA nanoparticles via anti-solvent precipitation in subcritical water, with detailed studies on the effects of operating parameters. The corresponding particle morphology, and dissolution rate properties of the CLA nanoparticles were characterized through scanning electronic microscopy (SEM), Fourier transform infrared spectrophotometry (FT-IR), powder X-ray diffraction (XRD) and dissolution tests. Under optimized experimental conditions, which was using 1.5 mL of SBCW at 150 °C as the solvent and 15 of aqueous PVP solution (0.4 wt%) as the anti-solvent, uniform sub-50 nm sized CLA nanoparticles are obtained. According to the dissolution testing, the ultrafine CLA nanoparticles exhibit very high dissolution rate (over 85% at 60 min) compared with that of raw CLA (10% at 60 min). Our results suggest that as-synthesized ultrafine CLA nanoparticles via anti-solvent precipitation in subcritical water are promising for efficient therapy.
© 2016 Published by Elsevier B.V.

1. Introduction

Clarithromycin (CLA), a broad-spectrum macrolide, is primarily used to treat various bacterial infections, such as strep throat, pneumonia, skin infections, Lyme disease, and just to name a few [1]. However, the poor water solubility of clarithromycin limits its effective bioavailability and absorption when administered orally. In nearly all cases, an oral drug must be dispersed well in solution to be absorbed into the bloodstream from the gastrointestinal tract [2]. Recent development in nanotechnology has provided a large variety of nanomaterials for diagnosis and therapy [3–6]. Nanonization of poorly water-soluble drugs has been demonstrated to be an efficient approach to overcome the limitations for low dissolution rate [7,8], and systemic side-effects [9]. Consequently, a variety of nanonization strategies for drugs have emerged, including high-pressure homogenization [10], mechanical comminution approach [11,12], anti-solvent precipitation [13–17], and sub- or supercritical fluid techniques [18–20].

Subcritical water (SBCW), which is held by pressure (up to 70 MPa) at a temperature (100–300 °C) higher than the natural boiling point (100 °C) of water, has been widely used as a solvent to extract a variety of organic compounds [21]. The SBCW technology has also been demonstrated to be capable of micronizing pharmaceuticals to synthesis micrometer-sized particles [22–25]. Recently, we have developed a green method for preparing ultrafine prednisolone nanoparticles by combining a subcritical water (SBCW) process with an anti-solvent precipitation [26].

In this work, we reported ultrafine CLA nanoparticles via anti-solvent precipitation in subcritical water, with detailed studies on the effects of operating parameters. The various processing parameters, such as the temperature of the SBCW solution, regular water (as anti-solvent), were investigated. Non-toxic and biocompatible PVP was used as stabilizers during the anti-solvent precipitation to prepare sub-50 nm sized CLA nanoparticles. The corresponding particle morphology, and dissolution rate properties of the CLA nanoparticles were characterized through scanning electronic microscopy (SEM), Fourier transform infrared spectrophotometry (FT-IR), powder X-ray diffraction (XRD) and dissolution tests. These results showed that as-synthesized CLA nanoparticles are promising for efficient therapy.

2. Experimental

2.1. Materials and instruments

The clarithromycin (≥99.53%, CAS No. 81103-11-9) was purchased from Guangdong Puhe Bio & Tech co., Ltd. The ethanol (≥99.75%, for washing) was purchased from Beijing Chemical Works. The nitrogen

* Corresponding author at: State Key Laboratory of Organic-Inorganic Composites, Beijing University of Chemical Technology, Beijing 100029, China.
E-mail address: wangdan@mail.buct.edu.cn (D. Wang).

http://dx.doi.org/10.1016/j.powtec.2016.09.073
0032-5910/© 2016 Published by Elsevier B.V.

(≥99.992%) was purchased from PREMER. The PVP K30 was obtained from Guangzhou Bolv Chemicals Co. Ltd. All the chemicals were used as received and deionized water prepared by a Hitech-K flow water purification system (Hitech instrument Co., Ltd. Shanghai, China) was used for all experiments.

The morphology studies were performed using a JEOL JSM-6360LV scanning electron microscope (SEM). Typically, a glass slide with the sample was fixed on an aluminum stub using double-sided adhesive tape and sputter coated with Au at 50 mA for 30 s by a Pelco Model 3 sputter-coater under an Ar atmosphere. The particle size distribution of the samples was determined by dynamic light scattering (DLS, Zetasizer, Malvern Instruments Ltd., UK). A PerkinElmer spectrum GX fourier transform infrared (FTIR) spectroscopy system was used to record the FITR spectra of solid samples. X-ray diffraction (XRD) patterns of the samples were measured by an XRD-6000 diffractometer (Shimadzu Inc., Japan), consisting of a rotating anode in transmission mode using Cu Kα radiation generated at 30 mA and 40 kV. The scanning speed was 5°/min in range of from 5° to 60° with a step size of 0.05°.

2.2. Setup of SBCW apparatus

The setup of SBCW apparatus is similar to our previous reports with some modifications [20]. A schematic diagram of the SBCW apparatus in this study is shown in Fig. 1. The fittings and tubing were composed of stainless steel (type 316). A 4848 Reactor Controller (Parr, USA) was attached to the 4590 Micro Bench Top Reactor (Parr, USA) to display the temperature, the pressure and the stirring speed of the system. Furthermore, the 4848 Reactor Controller was available with a microprocessor based control module that provided the precise temperature (±0.1 K) and the stirring speed control with adjustable tuning parameters. A Sartorious BSA224 electronic balance with a metering accuracy of ±0.1 mg was used to determine the masses of the relevant compounds.

2.3. Preparation of clarithromycin nanoparticles

Typically, the micro reactor (MR) had an internal volume of 6.4 mL and a 0.5-μm filter was installed inside the MR to remove any undissolved particles. For each run, the MR was loaded with 100 mg CLA and 1.5 mL water. The nitrogen used as protective gas was supplied to the system by a syringe pump (ISCO model 260D), which made the gas inside the MR reach 6 ± 0.01 MPa of pressure. V3 valve was left open during the supplying period, and after gas exhausted out for 5 min, V3 was closed. These conditions ensured that air was purged from the system. The system was brought to the selected temperature (e.g. 110 °C, 130 °C, 150 °C, 170 °C) using a heater which was controlled by the reactor controller, and the pressure was supplied by the nitrogen through V2. Once the set temperature was reached, the system was allowed to equilibrate while stirring at 160 rpm. After 25 min of mixing, the stirring was stopped. The system was maintained at a constant pressure (6 ± 0.01 MPa) by nitrogen gas, preventing the vaporization of the SBCW inside the apparatus during product collection. A nozzle with 1/8 in. OD stainless steel tubing was used to deliver the SBCW solution to the particles collection vial (PC). The flow from the MR to the precipitation vessel was controlled by valve V4. The saturated CLA solution was added to a PC containing 15 mL of water as the anti-solvent under constant magnetic stirring at 800 rpm for 3 min, forming dispersion of CLA nanoparticles. The powders of CLA nanoparticles were obtained by centrifugation (12,000 rpm for 15 min) of the suspension and dried in a vacuum oven at 60 °C. For the PVP-assistant synthesis of CLA nanoparticles, the experiment was performed in a similar way, except aqueous PVP solution (0.04, 0.08, 0.16, and 0.4 wt%, respectively) was used as the anti-solvent.

2.4. Dissolution testing

The dissolution tests for the drug powder were carried out using a dissolution apparatus (D-800LS, Tianjin, China) through the USP Apparatus II (paddle) method [27]. The paddle speed and bath temperature were set to 100 rpm and 37.0 ± 0.5 °C, respectively. A phosphate buffer (pH = 6.8) was used as the dissolution medium. Approximately 25 mg of CLA was placed into a vessel containing 900 mL of the dissolution medium. The samples (5 mL) were withdrawn at specific intervals (5 min, 10 min, 15 min, 20 min, 30 min, 45 min, 60 min, 90 min, 120 min, 150 min) and immediately filtered through a 450 nm syringe filter. Afterwards, the filtrate was injected into an ultraviolet spectrophotometer (Shimadzu, UV-2501, and Japan) operating at 290 nm. Each sample was analyzed in triplicate.

3. Results and discussions

3.1. Effect of the temperature of SBCW solutions

To investigate the effects of temperature to the synthesis of CLA nanoparticles, various experimental conditions were used to prepare the CLA nanoparticles (Table 1). Fig. 2 shows the corresponding SEM images of the unprocessed raw CLA drug (Fig. 2A) and CLA particles generated through the SBCW technology with different temperatures of SBCW solutions (Fig. 2 B–E). Compared with raw CLA, which had an irregular shape with a wide size distribution up to dozens of micrometers in length (Fig. 2A), the CLA precipitated from SBCW solution at 110 °C, crystallized to form rod-shaped particles that were 150–

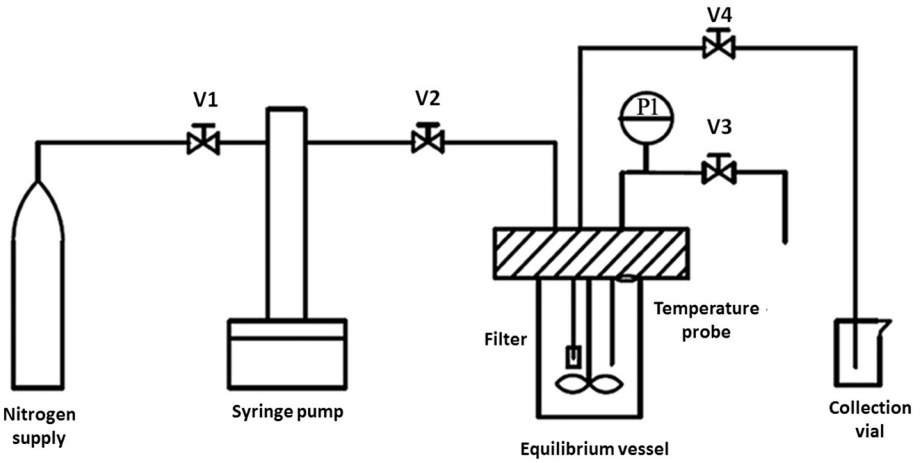

Fig. 1. Schematic diagram of subcritical water reactor system.

Table 1
Experimental conditions and results summary.

Experiment	Temperature of the solvent (°C)	Temperature of anti-solvent (°C)	Concentration of PVP (wt%)	Hydrodynamic diameter (nm)	Product morphology
1	110	20	0	N/A[a]	Rod-shape
2	130	20	0	N/A[a]	Sphere
3	150	20	0	~100	Sphere
4	170	20	0	~100	Sphere
5	150	0	0	~80	Sphere
6	150	40	0	~120	Sphere
7	150	20	0.04	~60	Sphere
8	150	20	0.08	~52	Sphere
9	150	20	0.16	~43	Sphere
10	150	20	0.4	~31	Sphere

[a] These samples were not suitable for DLS analysis due to the disturbing of large particles.

200 nm wide and up to dozens of micrometers in length (Fig. 2B). The CLA particles appear to be smaller when the SBCW solution temperature was increased from 110 °C to 130 °C (Fig. 2C). When 150 °C and 170 °C SBCW solutions were used, smaller spherical particles (100 nm in diameter) were precipitated (Fig. 2D and E).

The formation of CLA nanoparticles by the SBCW process were depicted in Fig. 3. After the mixing of CLA solution in SBCW and water, the solution was supersaturated with CLA molecules, and primary CLA particles formed through a burst-nucleation step. Subsequently, two kinds of growth modes for the growth of primary CLA particles

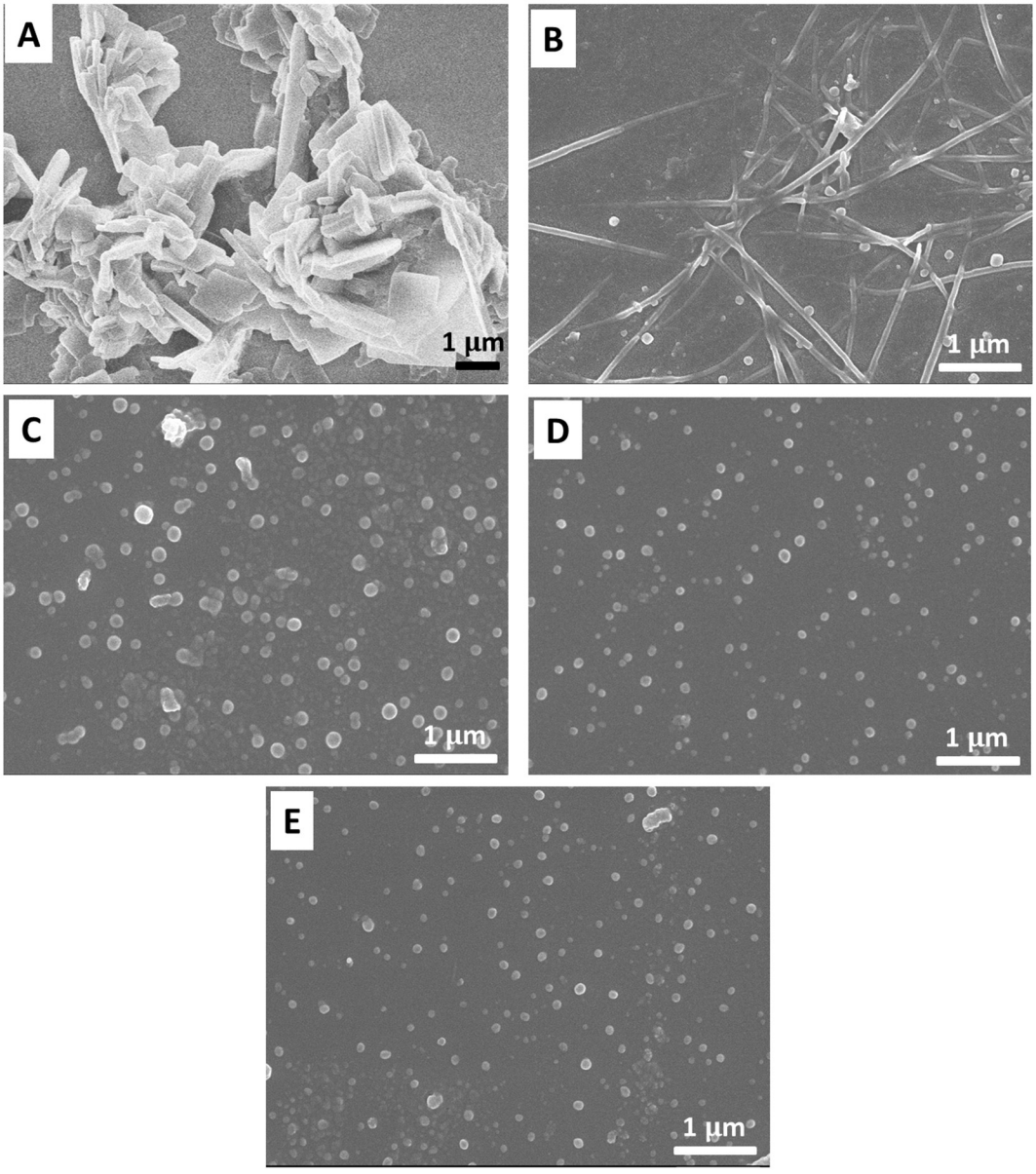

Fig. 2. SEM images of particles obtained from different temperatures of SBCW solutions and added into deionized water ($T = 20$ °C) :A 110 °C; B 130 °C; C 150 °C; D 170 °C.

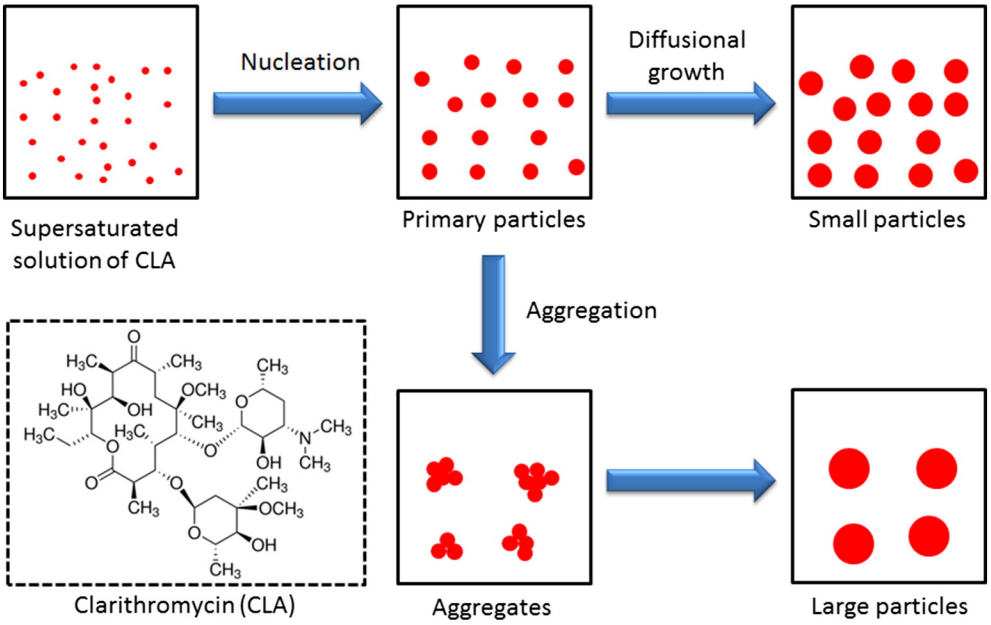

Fig. 3. Schematic diagram of the particle formation during the anti-solvent precipitation.

appeared: one was diffusional growth and the other was aggregation. It is generally accepted that within a short reaction time, the diffusional growth usually produces smaller particles than aggregation does [28]. For the preparation of CLA particles via SBCW process, the level of supersaturation was determined by the difference of the CLA solubility under subcritical and ambient water conditions. When the SBCW temperature was increased, the solubility of CLA began to increase, leading to an enhanced supersaturation, which resulting a decreased average particle size. In our experiment, when the temperature of SBCW increased to 170 °C, the obtained CLA nanoparticles did not shown significant difference with that of 150 °C. This was resulted by the combined effect of diffusional growth and aggregation route for the formation of CLA particles. The probability of particle collision increased drastically with increased temperature, leading to the aggregation and formation of large particles. Therefore, the enhancement of SBCW temperature over 150 °C did not result in smaller CLA particles, according to our experimental results, which suggested that the optimized temperature of SBCW used for the preparation of CLA nanoparticles was 150 °C when using water at room temperature as the anti-solvent.

3.2. Effect of temperature of the anti-solvent

Fig. 4 shows SEM images of CLA particles obtained by SBCW process with different temperature of the anti-solvent, while the temperature of

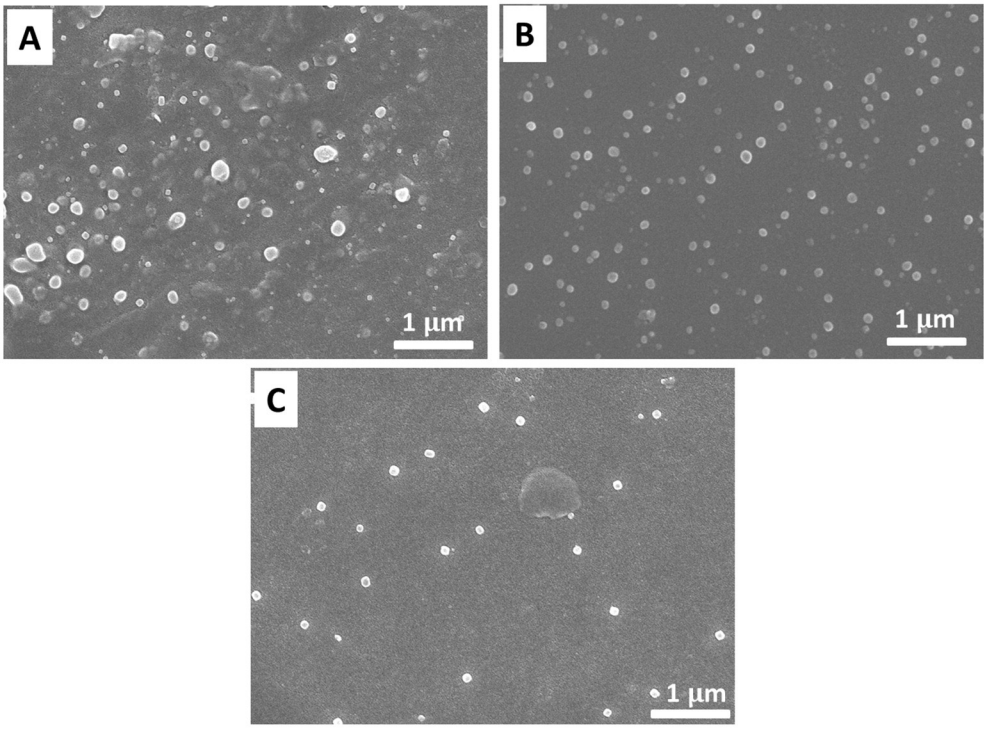

Fig. 4. SEM images of the CLA particles prepared using the anti-solvent at different temperatures A: 40 °C; B: 20 °C; C: 0 °C.

SBCW were constant at 150 °C. The CLA particles precipitated in the anti-solvent at 40 °C exhibit spherical morphology with larger size than those obtained from the anti-solvent of lower temperature (20 °C and 0 °C). According to the DLS measurement, the average hydrodynamic diameters of CLA nanoparticles were 100 nm and 80 nm when the temperature of anti-solvent were 20 °C and 0 °C respectively, which demonstrated that the lower precipitation temperature is more beneficial to the formation of uniform smaller particles. Since the temperature of SBCW was constant at 150 °C, the temperatures of the mixture from 1.5 mL of SBCW with 15 mL of water at 40, 20, and 0 °C were calculated to be approximate 50, 30 and 10 °C. The probability of particle collision increased drastically with increased temperature, which may lead to aggregation and formation of large particles. Therefore, the average size of CLA nanoparticles increased along with the increasing of anti-solvent temperature. Although low anti-solvent temperature was demonstrated to be beneficial in the preparation of small particles, it was noted that particles population generated from anti-solvent at 0 °C (Fig. 4C) was lower than particles obtained from anti-solvent at 20 °C (or 40 °C). We attributed this phenomenon to the following reason. According to previous reports [29,30], there was an inverse dependence of the solubility of CLA in pure water on temperature due to the hydrophobic hydration. Therefore, more CLA molecules precipitated when the anti-solvent temperature was 20 °C (or 40 °C) than that of 0 °C, resulting in higher yield of CLA nanoparticles. Comprehensive consideration of the size distribution, yields, and economy of the process, the use of anti-solvent at 20 °C was the optimal condition, compared with that of 0 °C and 40 °C.

3.3. Effect of the concentration of the pharmaceutical excipients PVP

Previous studies on poorly soluble drugs have demonstrated that particle size reduction can lead to an increased rate of dissolution and higher oral bioavailability [31]. Therefore, it is critical to develop ultrafine CLA particles (sub-100 nm) with high dissolution rate for oral applications. In this work, we performed PVP-assisted synthesis of CLA nanoparticles. Aqueous PVP solutions with different mass concentrations of 0.04 wt%, 0.08 wt%, 0.16 wt% and 0.4 wt% were used as the anti-solvents in the SBCW process to synthesize CLA nanoparticles, which were denoted as NanoCLA-A, NanoCLA-B, NanoCLA-C and NanoCLA-D. Fig. 4 presented the SEM images of CLA nanoparticles prepared by PVP-assisted anti-solvent precipitation in SBCW. The temperatures of SBCW and aqueous PVP solution were 150 °C and 20 °C respectively and all the NanoCLA/PVP particles were with diameters <100 nm. According to DLS measurement, the obtained CLA nanoparticles exhibited an average hydrodynamic diameter of 100 nm when the temperatures of SBCW and pure water were 150 °C and 20 °C (Fig. 5A). By adding 0.04 wt% PVP in water as the anti-solvent, CLA nanoparticles of with average diameters of 60 nm were obtained. According to the DLS results, the sizes of CLA nanoparticles were 52 nm, 43 nm, and 31 nm for NanoCLA-B, NanoCLA-C and NanoCLA-D. These results demonstrated that the PVP polymers effectively prevented the growth and aggregation of CLA nanoparticles in the SBCW process, leading to ultrafine particles. During the formation of CLA nanoparticles, the presence of PVP molecules adsorbed on the surface of the particles due to the hydrophobic bond, which enhanced the dispersion of CLA particles in the aqueous phase and limited the aggregation and growth of the CLA particles. Therefore, with the help of very small amount of PVP in the anti-solvent (0.04 wt%), ultrafine CLA nanoparticle could be prepared. When the PVP concentration was raised, there were enough PVP molecules to stabilize the CLA particles and the size decrease of obtained particles was no longer apparent.

In order to determine the component of CLA nanoparticles obtained by using PVP-assisted synthesis method, XRD and FTIR of raw CLA, raw PVP and NanoCLA/PVP were measured. According to the XRD patterns in Fig. 6B, the raw CLA drug exhibited many characteristic peaks, indicating the polycrystal structure. For the raw PVP, there were two broad peaks at 11° and 20°, respectively. However, from the XRD spectra of NanoCLA/PVP, no characteristic peaks from either CLA or PVP

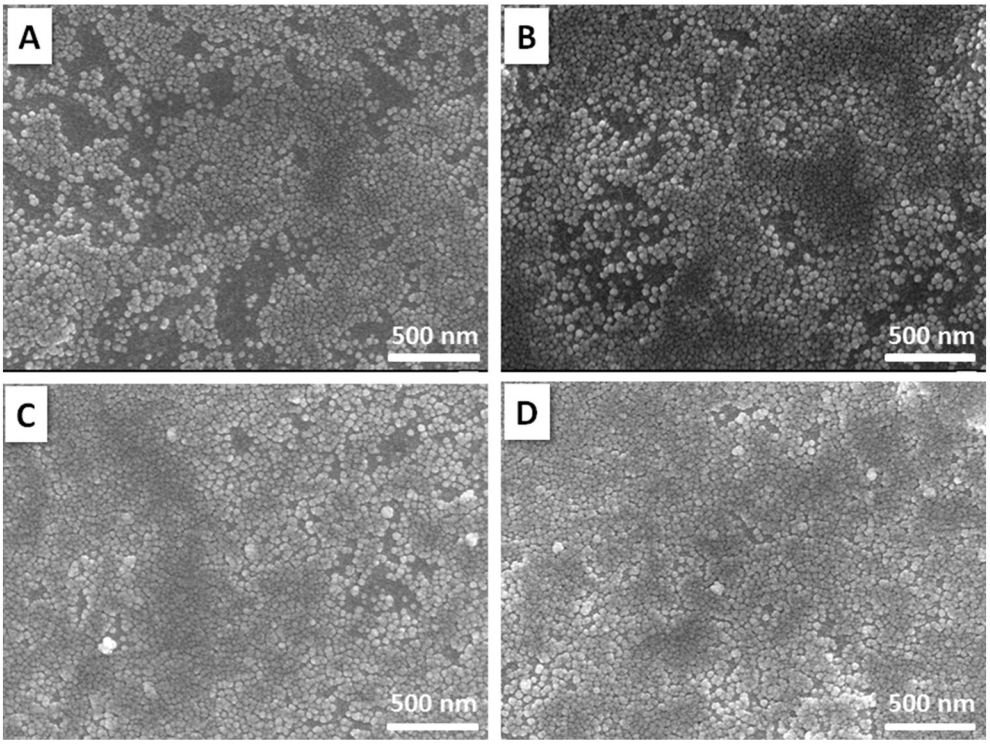

Fig. 5. SEM images of the CLA nanoparticles prepared by anti-solvent precipitation using 150 °C SBCW solutions and 20 °C aqueous PVP solutions with different concentrations (A) NanoCLA-A, PVP 0.04 wt%; (B) NanoCLA-B, PVP 0.08 wt%; (C) NanoCLA-C, PVP 0.16 wt%; (D) NanoCLA-D, PVP 0.4 wt%.

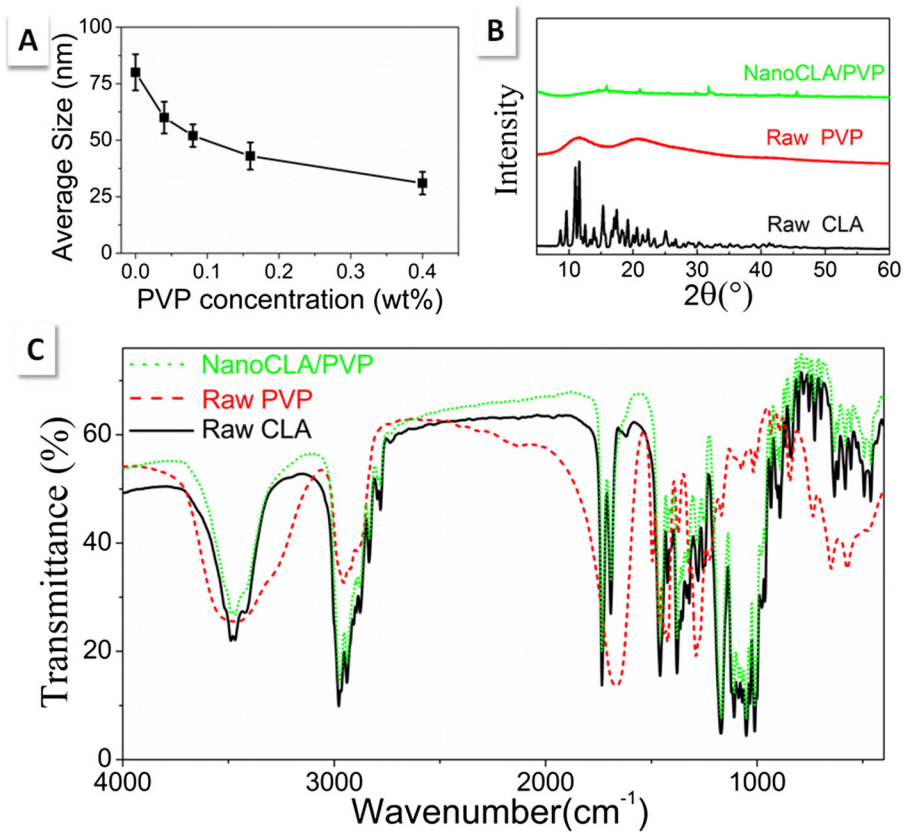

Fig. 6. (A) Hydrodynamic diameters of CLA nanoparticles prepared by anti-solvent precipitation using 150 °C SBCW solutions and 20 °C aqueous PVP solutions with different concentrations (0, 0.04, 0.08, 0.16 and 0.4 wt%) measured by DLS; (B) XRD patterns and (C) FTIR spectra of raw CLA, raw PVP, and NanoCLA/PVP.

were observed, which was attributed to the low crystallinity and ultrafine size. As shown in the FTIR spectra in Fig. 6C, the NanoCLA/PVP and raw CLA generated very similar FTIR spectra with same characteristic peaks, demonstrating that the SBCW process did not affect the chemical composition of CLA. The intensity of the –OH stretching vibration, $–CH_2–$ symmetrical and unsymmetrical stretching vibration of PVP molecules were hardly observed from the NanoCLA/PVP sample, suggesting that the content of PVP molecules absorbed on the surface of NanoCLA/PVP was very low. These results demonstrated that most of the PVP molecules were removed during experimental step of centrifugation to obtain powder of CLA nanoparticles. Since PVP was an agent approved food and drug administration (FDA) for clinical [32], the use of PVP-assisted synthesis of ultrafine CLA nanoparticles were important reference for practical applications.

3.4. Dissolution testing

The dissolution profiles of the raw CLA (Fig. 2A), submicron CLA particles (Fig. 2B), and ultrafine CLA nanoparticles (NanoCLA-D, Fig. 5D), were presented in Fig. 7. The submicron CLA particles (2B), and ultrafine CLA nanoparticles exhibited significantly higher dissolution rates than the raw drug. The dissolved amount of drug from submicron CLA and ultrafine CLA increased to 30.94% and 85.83%, respectively after 60 min, while only 10.58% of the raw CLA dissolved. After 150 min, approximately 31.11% and 88.83% of the submicron and ultrafine CLA dissolved, respectively, while only 10.58% of the raw drug dissolved. The highest dissolution rate of the ultrafine CLA nanoparticles was attributed to the smallest particle size. These results demonstrated that the reported SBCW process were able to ultrafine CLA nanoparticles with high dissolution rate, which should be beneficial for oral applications.

4. Conclusions

The uniform CLA nanoparticles were successfully prepared using the SBCW process. The effects of SBCW solution temperatures, anti-solvent temperatures and PVP mass concentrations on the mean particle size and size distribution of CLA were investigated. By increasing the SBCW solution temperature (up to 170 °C) and decreasing the anti-solvent temperature (down to 0 °C), ultrafine CLA nanoparticles with average size of 100 nm was obtained. Furthermore, PVP molecules were used as stabilizers and sub-50 nm sized CLA nanoparticles were prepared. Under optimized experimental conditions, which was using 1.5 mL of SBCW at 150 °C as the solvent and 15 of aqueous PVP solution

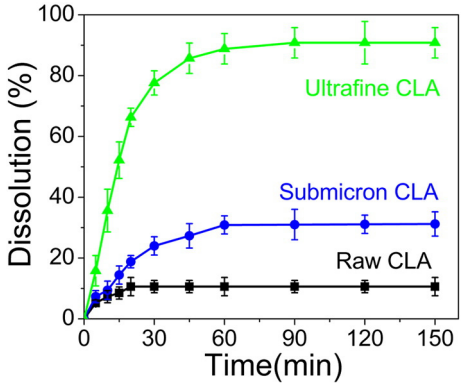

Fig. 7. Dissolution profiles of raw CLA, submicron CLA nanoparticles and ultrafine CLA nanoparticles.

(0.4 wt%) as the anti-solvent, uniform sub-50 nm sized CLA nanoparticles are obtained. Compared to the raw CLA powder, the ultrafine CLA particles exhibited similar chemical compositions, while the dissolution rate of the CLA particles was significantly enhanced due to the reduced size of particle. According to the dissolution testing, the dissolved amount of drug from NanoCLA/PVP nanoparticles in water was 85.83% after 60 min, while only 10.58% of the raw CLA dissolved. The SBCW process provides a green method of manufacturing CLA nanoparticles while controlling their size and morphology with potential application value.

Acknowledgements

We are grateful for financial support from the National Key R&D Program of China (2016YFA0201701 / 2016YFA0201700), National Natural Science Foundation of China (21306005), the Fundamental Research Funds for the Central Universities (BUCTRC201601, & JD1606), and the "111" project of China (B14004).

References

[1] S.C. Piscitelli, L.H. Danziger, K.A. Rodvold, Clarithromycin and azithromycin: new macrolide antibiotics, Clin. Pharm. 11 (1992) 137–152.
[2] M. Thanou, J.C. Verhoef, H.E. Junginger, Oral drug absorption enhancement by chitosan and its derivatives, Adv. Drug Deliv. Rev. 52 (2001) 117–126.
[3] D. Wang, J.-F. Chen, L. Dai, Recent advances in graphene quantum dots for fluorescence bioimaging from cells through tissues to animals, Part. Part. Syst. Charact. 5 (2015) 515–523.
[4] D. Wang, L. Zhu, J.-F. Chen, L. Dai, Can graphene quantum dots cause DNA damage in cells, Nanoscale 7 (2015) 9894–9901.
[5] D. Wang, L. Zhu, C. McCleese, C. Bruda, J.-F. Chen, L. Dai, Fluorescent carbon dots from milk by microwave cooking, RSC Adv. 6 (2016) 41516–41521.
[6] D. Wang, L. Zhu, J.-F. Chen, L. Dai, Liquid marbles based on magnetic upconversion nanoparticles as magnetically and optically responsive miniature reactors for photocatalysis and photodynamic therapy, Angew. Chem. Int. Ed. 55 (2016) 10795–10799.
[7] V.B. Patravale, A.A. Date, R.M. Kulkarni, Nanosuspensions: a promising drug delivery strategy, J. Pharm. Pharmacol. 56 (2004) 827–840.
[8] F. Kesisoglou, S. Panmai, Y. Wu, Nanosizing-oral formulation development and biopharmaceutical evaluation, Adv. Drug Deliv. Rev. 59 (2007) 31–44.
[9] K. Riehemann, S.W. Schneider, T.A. Luger, B. Godin, M. Ferrari, H. Fuchs, Nanomedicine-challenge and perspectives, Angew. Chem. Int. Ed. 48 (2009) 872–897.
[10] C.M. Keck, R.H. Müller, Drug nanocrystals of poorly soluble drugs produced by high pressure homogenization, Eur. J. Pharm. Biopharm. 62 (2006) 3–16.
[11] M.D. Louey, M.V. Oort, A.J. Hickey, Aerosol dispersion of respirable particles in narrow size distributions produced by jet-milling and spray-drying techniques, Pharm. Res. 21 (2004) 1200–1206.
[12] N. Rasenack, H. Steckel, B.W. Müller, Micronization of anti-inflammatory drugs for pulmonary delivery by a controlled crystallization process, J. Pharm. Sci. 92 (2003) 35–44.
[13] Z. Wang, J.F. Chen, Z.G. Shen, J. Yun, Preparation of ultrafine beclomethasone dipropionate drug powder by antisolvent precipitation, Ind. Eng. Chem. Res. 46 (2007) 4839–4845.
[14] X.S. Li, J.X. Wang, Z.G. Shen, P.Y. Zhang, J.F. Chen, J. Yun, Preparation of uniform prednisolone microcrystals by a controlled microprecipitation method, Int. J. Pharm. 342 (2007) 26–32.
[15] D. Wang, J. Qian, F. Cai, S. He, S. Han, Y. Mu, 'Green' synthesized near-infrared PbS quantum dots with silica-PEG dual-layer coating: ultrastable and biocompatible optical probes for in vivo animal imaging, Nanotechnology 23 (2012) 245701.
[16] D. Wang, J. Qian, S. He, J.S. Park, K.-S. Lee, S. Han, Y. Mu, Aggregation-enhanced fluorescence in PEGylated phospholipid nanomicelles for in vivo imaging, Biomaterials 32 (2011) 5880–5888.
[17] J. Liu, D. Wang, M. Wang, D. Kong, Y. Zhang, J.-F. Chen, L. Dai, Uniform two-dimensional Co3O4 porous sheets: facile synthesis and enhanced photocatalytic performance, Chem. Eng. Technol. 39 (2016) 891–898.
[18] P. Chattopadhyay, R.B. Gupta, Production of griseofulvin nanoparticles using supercritical CO_2 antisolvent with enhanced mass transfer, Int. J. Pharm. 228 (2001) 19–31.
[19] S.V. Dalvi, M. Mukhopadhyay, A novel process for precipitation of ultra-fine particles using sub-critical CO_2, Powder Technol. 195 (2009) 190–195.
[20] F. Masoodiyeh, J. Karimi-Sabet, A.R. Khanchi, M.R. Mozdianfard, Zirconia nanoparticle synthesis in sub and supercritical water-particle morphology and chemical equilibria, Powder Technol. 269 (2015) 461–469.
[21] S. Deguchi, M. Ogawa, W. Nowak, M. Wesolowska, S. Miwa, K. Sawada, J. Tsuge, S. Imaizumi, H. Kato, K. Tokutake, Y. Niihara, N. Isu, Development of super- and subcritical water annealing processes, Powder Technol. 249 (2013) 163–167.
[22] A.G. Carr, R. Mammucari, N.R. Foster, Solubility and micronization of griseofulvin in subcritical water, Ind. Eng. Chem. Res. 49 (2010) 3403–3410.
[23] A.G. Carr, R. Mammucari, N.R. Foster, Particle formation of budesonide from alcohol-modified subcritical water solutions, Int. J. Pharm. 405 (2011) 169–180.
[24] S.K. Poornachary, G. Han, J.W. Kwek, P.S. Chow, R.B.H. Tan, Crystallizing micronized particles of a poorly water-soluble active pharmaceutical ingredient: nucleation enhancement by polymeric additives, Cryst. Growth Des. 16 (2016) 749–758.
[25] W.H. Teoh, R. Mammucari, S.A.B.V. de Melo, N.R. Foster, Solubility and solubility modeling of polycyclic aromatic hydrocarbons in subcritical water, Ind. Eng. Chem. Res. 52 (2013) 5806–5814.
[26] X.-Y. Chen, Y.-L. Shang, Y.-H. Li, J.-X. Wang, A.G. Maimouna, Y.-X. Li, D. Zou, N.R. Foster, J. Yun, Y. Pu, Green preparation of uniform prednisolone nanoparticles using subcritical water, Chem. Eng. J. 263 (2015) 20–26.
[27] H.X. Zhang, J.X. Wang, Z.B. Zhang, L. Yuan, Z.G. Shen, J.-F. Chen, Micronization of atorvastatin calcium by antisolvent precipitation process, Int. J. Pharm. 374 (2009) 106–113.
[28] J. Park, V. Privman, E. Matijevic, Model of formation of monodispersed colloids, J. Phys. Chem. B 105 (2001) 11630–11635.
[29] Y. Nakagawa, S. Itai, T. Yoshida, T. Nagai, Physicochemical properties and stability in the acidic solution of a new macrolide antibiotic, clarithromycin, in comparison with erthyomycin, Chem. Pharm. Bull. 40 (1992) 725–728.
[30] Z. Wang, J. Wang, M. Zhang, L. Dang, Solubility of erythromycin A dihydrate in different pure solvents and acetone + water binary mixtures between 293 K and 323 K, J. Chem. Eng. Data 51 (2006) 1062–1065.
[31] J. Hu, K.P. Johnston, R.O. Williams III, Nanoparticle engineering processes for enhancing the dissolution rates of poorly water soluble drugs, Drug Dev. Ind. Pharm. 30 (2004) 233–245.
[32] K. Sokolov, M. Follen, J. Aaron, I. Pavlova, A. Malpica, R. Lotan, R. Richards-Kortum, Real-time vital optical imaging of precancer using anti-epidermal growth factor receptor antibodies conjugated to gold nanoparticles, Cancer Res. 63 (2003) 1999–2004.